2011 NDIA GROUND VEHICLE SYSTEMS ENGINEERING AND TECHNOLOGY SYMPOSIUM
POWER AND MOBILITY (P&M) MINI-SYMPOSIUM
AUGUST 9-11 DEARBORN, MICHIGAN

Tailoring of Acoustic, Smoke and Thermal Signatures from Diesel-Powered Unmanned Ground Vehicles

Marcis Jansons
Sukhbir Khaira
Walter Bryzik
Department of Mechanical Engineering
Wayne State University
Detroit, MI

ABSTRACT

This work investigates non-traditional operating modes of a diesel engine that allow the tailoring of acoustic, smoke and thermal signatures for unique unmanned ground vehicle (UGV) military applications. A production, air-cooled single-cylinder diesel engine having a mechanical fuel injection system has been retrofit with a flexible common-rail injection and electronic control system. The experimental domain explores the effects of the injection timing and pressure on the engine's acoustic, smoke and heat signatures through analysis of the in-cylinder combustion processes. Surface maps of loudness, exhaust temperature and exhaust smoke density over the range of fuel injection strategies are presented, illustrating the degree to which each signature may be controlled. Trade-offs between the signature modes are presented and discussed. The results demonstrate the possibility of providing military UGVs the capability to tailor their acoustic, infrared and smoke signatures independent of speed and load, through an injection system retrofit and control strategy.

INTRODUCTION

The ability to tailor acoustic, infrared and smoke emission signatures is a desirable characteristic of a military unmanned ground vehicle (UGV) or auxiliary power unit (APU). Military missions in urban areas among civilian populations present a need for effective, remote, non-lethal weapons. Generating acoustic waves with intensities exceeding the human threshold of pain, Long-Range Acoustic Devices (LRADs) devices (American Technology Corporation) have been fielded for this purpose by the US military. Likewise, smoke generators may also be suitable for crowd dispersal or reducing visibility. The production of intense infrared (IR) signatures by UGVs can be utilized as a decoy to deflect heat-seeking missiles away from manned or otherwise higher-value targets. Conversely, sentinel duty may require quiet operation with reduced IR and visible smoke signatures.

Developments in commercial diesel engine technology such as common rail and variable high-pressure injection systems present a heretofore unachievable degree of control over the combustion process. Parameters which may be manipulated include cylinder gas pressures, their rise rates, in-cylinder and exhaust temperatures, and particulate emissions. This project evaluates non-traditional operating modes of a light-duty diesel engine suitable for use in UGVs, which allow the tailoring of their acoustic, thermal and soot signatures.

Combustion-generated engine noise is the result of rapid in-cylinder pressure rise which drives the combusting gas volume into acoustic resonance. The engine structure is induced to vibrate by these pressure oscillations, and further radiates pressure waves external to the engine as noise.

The intensity I, or power flux, of the harmonic waves which act as the noise source has been quantified and related to in-cylinder parameters by Eng [1] through:

$$I = \frac{1}{2\gamma}\frac{\Delta P^2}{P}\sqrt{\gamma RT} \qquad 1)$$

Where P is the gas pressure, γ the ratio of specific heats, R the gas constant, T the gas temperature and a pressure pulsation amplitude, ΔP, defined by the product of an empirical scale factor β which relates the maximum tine rate

of pressure rise, $\frac{dP}{dt_{Max}}$ to the observed pressure oscillations in the cylinder:

$$\Delta P = \beta \frac{dP}{dt_{Max}} \quad 2)$$

The dominant parameter in the above relations is the rate of cylinder pressure change, with the intensity attenuated by an inverse relationship with the magnitude of the cylinder pressure.

While multiple resonance frequencies can be calculated for particular engine geometry [2], cylinder pressure oscillation energy has been found to be dominated by the first circumferential mode [1,3], the characteristic frequencies of which are on the order of 5 kHz. This value is determined largely by geometry (bore or bowl diameter), and combustion temperature, roughly corresponding to typical values of 85mm and 2500K, respectively. Cylinder pressure oscillations have been observed to occur at the same frequencies in a spark-ignition (SI) engine under both normal and knocking operation [4]. Such results indicate that audible noise levels are not determined by variation in the frequency distribution, but rather by changes of oscillation intensity at the characteristic frequencies of a given engine. Historically efforts have been aimed at minimizing engine noise [5,6].

The electro-magnetic emission of a gas volume may be described by a wavelength, λ, and temperature, T, -dependent emissivity, $\epsilon(\lambda, T)$, which modifies Planck's blackbody function, I_{bb}, as:

$$I(\lambda, T) = \varepsilon(\lambda, T) I_{bb} = \varepsilon(\lambda, T) \frac{C_1}{\lambda^5 \left(exp\left(\frac{C_2}{\lambda T}\right) - 1\right)} \quad 3)$$

Where C_1 and C_2 are the first and second radiation constants.

At a given temperature, the continuous blackbody function, I_{bb}, has a peak intensity at a wavelength λ_{Peak}, which according to Wien's Displacement Law occurs:

$$\lambda_{Peak} T = 2{,}898\ \mu m \cdot K \quad 4)$$

As the exhaust gas temperature of an engine is varied from 500 to 800K, the peak emission shifts from near 6 μm to 3.6 μm. This range falls in the mid-IR range of the spectrum, and covers the strong 4.3 μm carbon dioxide band expected to be present in hydrocarbon combustion products. This range also coincides with optimum responsivity ranges of common Mercury-Cadmium Telluride (HgCdTe) and Indium Antimonide (InSb) detectors commonly used in night-vision or heat-seeking devices.

While the thermal efficiencies of diesel engines may be in the range of 40-50%, [7] and indicating the fraction of input fuel energy extracted as mechanical work, the balance of the energy input becomes a heat flux across engine or radiator surfaces and the exhaust stream. The distribution of heat flux between the exhaust and cooling system, however, may vary greatly depending on operating condition. Donn *et al* [8] have measured the exhaust heat flux of a commercial diesel engine under light load to be 12% at a low load and speed and cooled EGR condition, which then rises to 32% at a high speed and medium load without EGR. Since heat flux from engine and radiator surfaces typically occurs at the temperatures of the coolant, typically near 100C, the greatest IR signature intensity is produced by the engine exhaust gases the temperatures of which typically exceed this value.

Engine-out soot emission from a diesel engine has been described as the net result of the in-cylinder soot formation and oxidation process. Soot emissions are generally produced under conditions where local equivalence ratios exceed 2.4 and temperatures lie between 1700 and 2100K [9,10]. Stringent emissions regulations have focused much attention to soot formation mechanisms and reduction techniques. Well-documented approaches include various combinations of reducing combustion temperatures or equivalence ratios to fall outside the above ranges.

Exhaust smoke levels are commonly measured by observing the degree of extinction of a visible, green (~750nm) light beam traversing an exhaust gas volume. The source intensity, I_0, is related to the attenuated intensity, I, detected by a sensor along a path in the gas volume through Beer's Law:

$$I = I_0 e^{-n\overline{aQ}L} \quad 5)$$

Where n is the soot particle number density, $\bar{a}$ is the average particle projected area, $\bar{Q}$ the average particle extinction coefficient and L the pathlength between the source and detector. In practice, smoke meter output is calibrated in terms of a smoke density parameter, K, lumping together the former three terms:

$$K = n\overline{aQ} \quad 6)$$

This work experimentally examines the degree to which the acoustic, infrared and smoke signature of a light-duty diesel engine can be manipulated through choice of start-of-injection, or injection timing, and injection pressure while maintaining a medium speed and load. An off-the shelf, light-duty, air-cooled single-cylinder diesel engine is retrofit with a common rail injection system to provide control of these parameters. The acoustic, infrared and smoke signatures of the engine are mapped over a range of injection

timings and injection pressures, from which trade-offs are determined.

EXPERIMENTAL SETUP

Experiments were performed on a naturally aspirated, 10.3 kW, single-cylinder 0.67-liter displacement air-cooled diesel engine having the specifications shown in Table 1. This engine is typical of a class suitable for light-duty operation in a UGV or APU. The stock mechanical injection system of this engine has been converted to an electronically-controlled common rail system, where an external electric motor is used to drive the high pressure fuel pump. The nozzle of the electrically-controlled injector used during the experiment is custom fabricated to maintain the spray orientation of the original mechanical injector, and to contain the fuel spray within the re-entrant type piston bowl.

The engine is connected to a hydraulic dynamometer (with absorbing capacity of 47.5 N-m torque) which is acoustically isolated with acoustic foam. The in-cylinder pressure was monitored with a piezoelectric water-cooled pressure transducer (Kistler 6061B) having a measuring range of 0-250 bars, natural frequency 90 KHz and a sensitivity of -25pC/bar. The pressure transducer signal is amplified by a dual-mode charge amplifier (Kistler 5010B) whose output is recorded with a data acquisition system at 0.2 crank-angle degree intervals.

Table 1: Engine specifications

Manufacturer:	Hatz
Model:	1D81
No. cylinders:	1
Bore x Stroke:	100x85 mm
Displacement:	0.667 L
Connecting Rod Length:	190mm
Compression Ratio:	20.5
Max Power @3000RPM:	10.3 kW
Max Power @2600RPM:	9.5 kW
Max Power @2350RPM:	8.9 kW
Mean Piston Speed @3000 RPM:	8.5 m/sec
Injection:	Direct
Injector Holes x Diameter	6 x162µm
Injector Flow	450cc/30 sec @100 bar

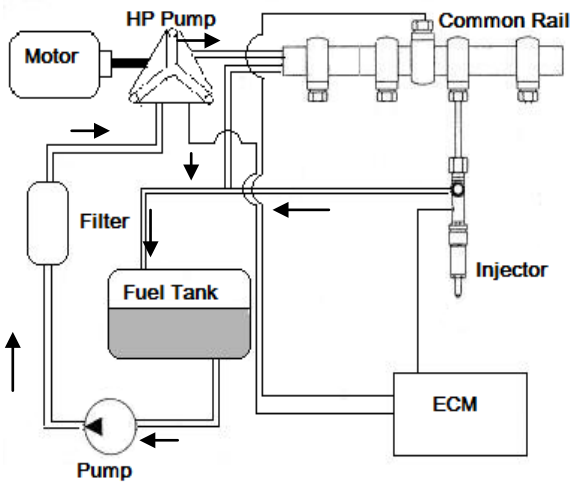

Figure 1: Common Rail Injection Unit.

Engine noise was recorded by three condenser microphones located 120 degrees apart in a plane normal to the cylinder bore at a distance of 1 m from the engine and at the elevation of the cylinder head. The microphone signals were analyzed for loudness and frequency content by Fourier Transform (National Instruments Labview). Loudness is reported in this work in units of Phons, the sound intensity detected by the microphones weighed by frequency-dependent sensitivity of human hearing. Data acquisition from the microphone signals were obtained on a time basis at a maximum sampling rate of 51.2 kS/s per channel and with a dynamic range of 102 dB. While mechanical sources such as piston slap and valve train impacts are well known to significantly contribute to overall engine noise, this study is focused on the effects of combustion noise that may be controlled through choice of injection parameters.

The smoke levels in the exhaust were measured with a water-cooled opacity meter (Telonic Berkeley) placed in the exhaust line roughly two feet downstream from the exhaust port. Exhaust temperatures from which infrared intensities were calculated were measured with thermocouples directly downstream of the exhaust port.

Experiments were conducted under steady conditions over a range of injection timings and injection pressures. Speed and brake torque were held constant to represent conditions where the engine is expected to maintain load, with injection duration adjusted to offset thermal efficiency variations caused by the varied injection timing. While speed and load values clearly impact noise, exhaust temperature and smoke levels, this study addressed the role of injection settings. Standard Ultra-Low Sulfur Diesel (ULSD) fuel was used for all experiments.

RESULTS

Loudness level variation over a range of injection timings from 5 to 25 degrees before top-dead center (bTDC) and over a range of injection pressures from 250 to 700 bars, while maintaining 10 N-m output torque (1.9 bar bMEP) and a speed of 1500 RPM are shown in Figure 2. Engine loudness increases with injection pressure and advanced injection timing, with the greatest intensity observed with advanced, high-pressure injection. Conversely, retarded, low-pressure injection resulted in the most quiet engine operation. Under the conditions examined, loudness may be modified by over seven Phons through choice of injection parameters while maintaining speed and load. The greatest sensitivity of loudness to injection advance occurs at the higher injection pressures, where at 700 bar, a rise in loudness of 3 Phons occurs when the start of injection (SOI) is advanced form 5 to 17 degrees bTDC. The same 3 Phon increase requires greater advance, from 5 to 25 °bTDC at the lower injection pressure of 250 bar. SOI is determined as the timing of the current pulse to the fuel injector solenoid which precedes actual needle opening by a time lag on the order of one degree.

Exhaust temperatures are mapped over the same range of injection timing and pressure and shown in Figure 3. The lowest temperatures occur at high injection pressures at an SOI near 12 °bTDC. As injection timing deviates from this value, through both advancing and retarding directions, exhaust temperature increases. Exhaust temperature shows both the greatest magnitude and sensitivity at retarded, low-pressure injection. Variations in exhaust temperature may be obtained from 230 to 303 °C over the range of injection parameters examined here.

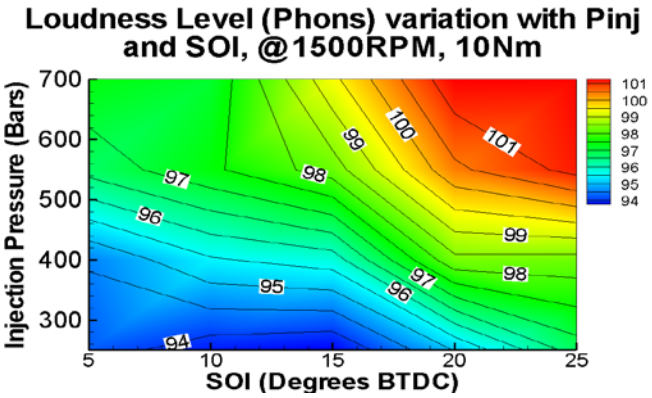

Figure 2: Loudness Map

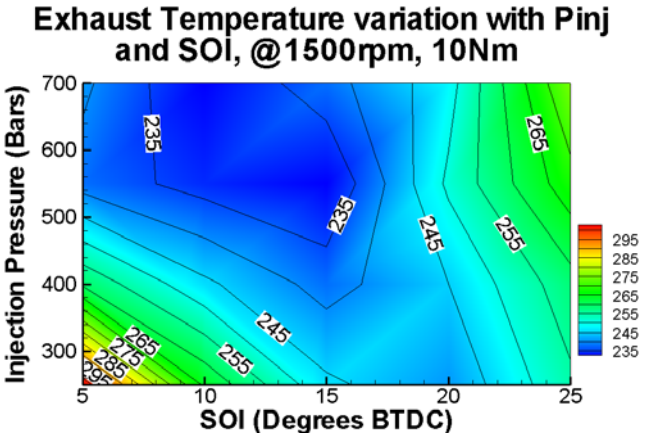

Figure 3: Exhaust Temperature Map

Figure 4 shows the effect of injection pressure and SOI on exhaust smoke levels. The greatest values occur at low injection pressure at an SOI near 10 °bTDC, and decreasing at all injection timings as the injection pressure is raised to 400 bar. As the injection pressure is further raised, smoke production increases, at a rate greatest at retarded injection timings. At all injection timings, smoke levels are at a minimum at 400 bar injection pressure. The increase in soot levels above this pressure are believed to result from corresponding increase in liquid fuel jet penetration length and subsequent wall fuel wetting in the small-diameter piston bowl. This is expected to lead to diffusion pool burning along the bowl periphery and greater soot production.

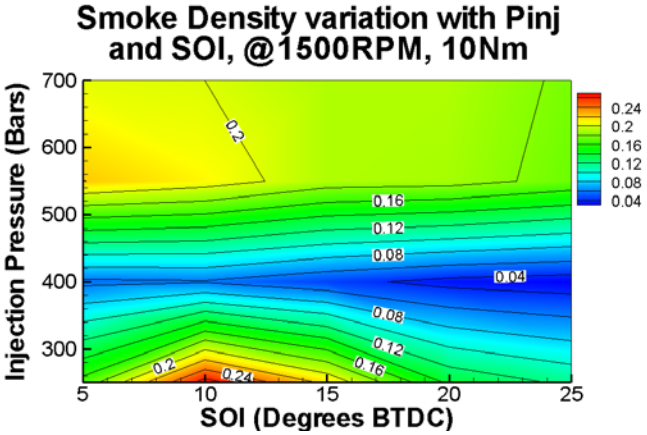

Figure 4: Exhaust Smoke Map

The combustion behavior leading to the loudness, exhaust temperature and soot production mapped in Figures 2-4 is examined through analysis of cylinder pressure and injector needle lift traces obtained by averaging data from 100 consecutive engine cycles under steady operating conditions.

Figure 5 shows the cylinder pressures over a start-of-injection sweep. At an SOI of 5 °bTDC, peak cylinder pressure is 58 bars, which rises to 84 bars when the SOI is advanced to 25 °bTDC. This effect is accompanied by a concurrent increase in the rate of pressure rise upon ignition. For SOI of 15, 20 and 25 °bTDC, ignition, marked by the inflection point in the pressure trace, occurs prior to TDC, and heat release occurs while the piston is still imparting work on the gas volume at the end of the compression stroke. Bulk gas temperatures thus increase as the SOI is advanced. The higher rate of cylinder pressure change, together with higher temperatures characteristic of advanced SOI dominate the expressions of Equations 1) and 2), leading to higher ringing intensity and loudness observed in the microphone signals. Examination of the combustion phasing, as indicated by a positive pressure rise rate subsequent to ignition, illustrates that 10 °bTDC SOI timing releases energy closest to TDC, allowing the greatest degree of expansion and work extraction. This coincides with the SOI of least exhaust gas temperature shown in Figure 3. For an SOI of 5 °bTDC, Figure 5 shows ignition to occur prior to the end of the injection event, indicating fuel is injected into active combustion zones and explaining the increased soot production at these conditions. Owing to lower compression temperature at the advanced SOI of 25 °bTDC, ignition delay is longer than the injection event, leading to greater accumulation and mixing of vaporized fuel, increased rates of pressure rise and reduced soot formation.

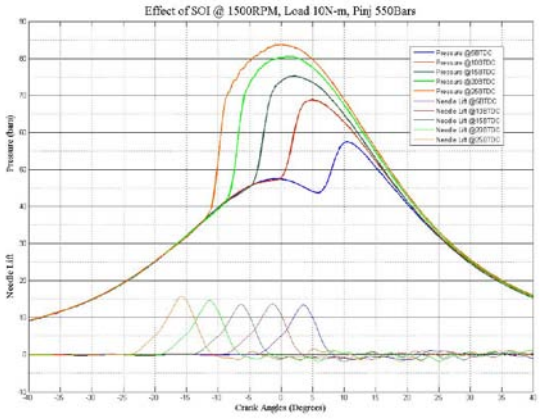

Figure 5: Effect of Injection Timing on Cylinder Pressure.

Figure 6 shows the injector needle lift and cylinder pressures for a sweep of injection pressures while maintaining a constant SOI of 5 °bTDC. Clearly, fuel injection duration increases as the injection pressure is decreased. At an injection pressure of 700 bar, the injector needle is fully closed by 7 °aTDC, while at 250 bar injector pressure this event occurs seven degrees later at 14 °aTDC. At depressed injection pressures, the slow rate of fuel delivery, together with decreased fuel atomization, leads to the aforementioned situation where fuel injection continues into active combustion zones leading to greater soot production. Higher injection pressures enhance atomization and evaporation rates, leading to shorter ignition delay. Upon ignition, the greater degree of premixing results in reduced soot levels and rapid heat release. For the conditions shown, as injection pressure is raised, greater pressure rise rates, higher bulk temperatures and high values of ringing intensity (Eq. 1, 2) result, leading to greater loudness seen in figure 3. The shorter ignition delay also leads to heat release occurring closer to TDC, allowing a greater fraction of the energy contained within the gas volume to be extracted as mechanical work and yielding lower exhaust temperatures.

The family of curves in Figure 7 shows the trade-offs between exhaust gas temperature and acoustic noise. Each line represents an injection pressure, with the data points along each line corresponding to different SOI timings. The lines form an envelope of loudness and exhaust temperature values which may be achieved through choice of injection parameters. Higher loudness levels require higher injection pressures, while the highest exhaust temperatures and lowest loudness levels are achieved with low injection pressure. Within the signal envelope, multiple combinations of injection pressure and SOI exist which satisfy a given loudness and exhaust temperature requirement, allowing the optimization of this choice with respect to a third parameter.

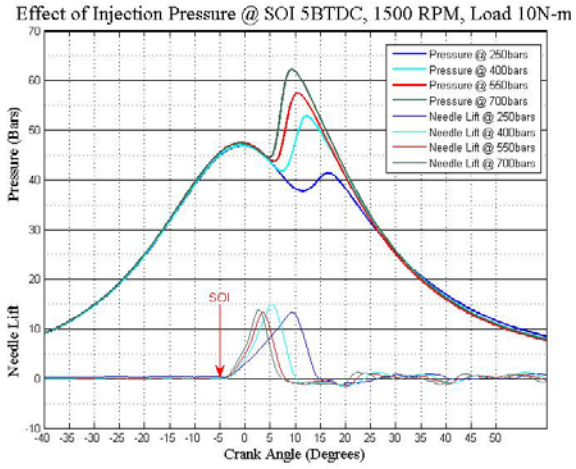

Figure 6: Effect of Injection Pressure on Cylinder Pressure

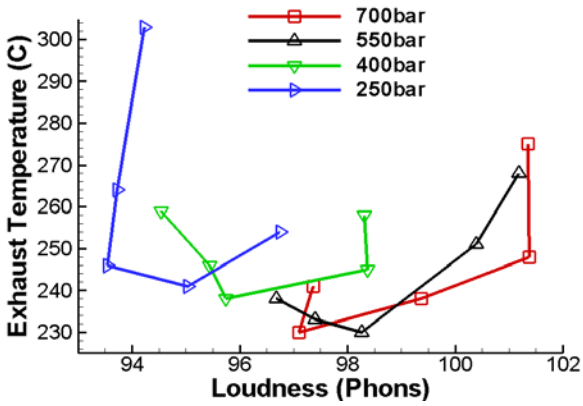

Figure 7: Exhaust Temperature and Loudness Tradeoffs as a Function of Start-of-Injection and Injection Pressure

CONCLUSIONS

The ability to tailor the acoustic, infrared and smoke signatures of a light-duty single-cylinder air-cooled diesel engine through choice of injection strategy, independent of speed and load, has been examined and demonstrated. Retrofitting of the mechanical injection system of the commercial engine with an electronically-controlled common rail alternative provided the degrees of freedom requisite for manipulating ignition delay, cylinder pressure rise rate, combustion phasing and duration and ringing intensity. Acoustic, infrared and smoke signatures were mapped over a range of injection timings and injection pressures for a single injection with the engine held at a constant speed and load.

The greatest engine combustion noise is found to be generated by conditions producing high cylinder pressure rise rates, high gas temperature and elevated ringing intensity. These are observed under advanced start of injection and high injection pressure conditions which allow a large degree of fuel-air premixing prior to autoignition before TDC. Observed loudness levels were lowest under retarded injection timing and low injection pressure, which result in low cylinder pressure rise rates, low bulk temperature and low premixed burn fraction.

Exhaust temperatures, and hence IR signatures, are least when combustion is brief and occurs closest to TDC. This condition is achieved with a high injection pressure and a start of injection near 10 °bTDC, which maximizes the expansion of the combusted gases. While injection timings both advanced and retarded from this value increase exhaust temperature, the degree of injection advance is limited by elevated cylinder pressure resulting from heat release during compression. The greatest exhaust temperature is thus obtained with retarded injection timing and low injection pressure.

Engine-out soot levels are minimized by enhancing premixing through higher injection pressures or extending ignition delay through advanced timing. However, further increase of injection pressure beyond 400 bar led to slight increase in soot levels attributed to greater liquid penetration and wall wetting by the fuel jet. Maximum soot levels were observed at low injection pressure and injection timings resulting in shortest ignition delay, where fuel is deposited into active combustion zones.

The trade-offs between acoustic and infrared signatures have been determined, establishing an envelope of loudness and exhaust temperature that may be realized by choice of injection parameters. However, further examination and optimization of multiple injection strategies is expected to significantly extend the degree of control over these signatures and expand the range of loudness, exhaust temperature and smoke-generating capabilities.

The successful implementation of signature-controlled diesel combustion may enhance the tactical mission capabilities of UGVs, allowing them to be used as IR decoys, smoke generators, or non-lethal weapons for crowd dispersal. UGV survivability may be also be enhanced by a reduction in such signatures.

ACKNOWLEDGEMENTS

The authors gratefully acknowledge the support of Dr. Matthew Castanier, US Army TARDEC, and the Ground Robotics and Reliability Center.

REFERENCES

1. Eng, J. A., "Characterization of Pressure Waves in Hcci Combustion", SAE Paper No. 2002-01-2859, 2002.
2. Scholl, D., Davis, C., Russ, S. and Barash, T., "The Volume Acoustic Modes of Spark-Ignited Internal Combustion Engines", SAE Paper No. 980893, 1998.
3. Hickling, R., Feldmaier, D. A., Chen, F. H. K. and Morel, J. S., "Cavity Resonances in Engine Combustion Chambers and Some Applications", The Journal of the Acoustical Society of America, **73** (4), pg. 1170-1178, 1983.
4. Leppard, W. R., "Individual-Cylinder Knock Occurence and Intensity in Multicylinder Engines", SAE Paper No. 820074, 1982.
5. Kubota, S., Takeda, N. and Furubayashi, M., "Vehicle Noise with Small Diesel Engine", SAE Paper No. 765035, 1976.
6. Thien, G. E., "A Review of Basic Design Principles for Low-Noise Diesel Engines", SAE Paper No. 790506, 1979.

7. Reitz, R. in: *Fuel Reactivity Controlled Compression Ignition (Rcci) - a Practical Path to High-Efficiency, Ultra-Low Emission Internal Combustion Engines*, SAE High Efficiency IC Engines Symposium, Detroit, MI, 2011; Detroit, MI, 2011.
8. Donn, C., Zulehner, W., Ghebru, D., Spicher, U. and Hontzen, M., "Experimental and Numerical Heat Flux Analysis Using a State-of-the-Art Passenger Car Diesel Engine During Warm-up and Steady-State Operation ", SAE Paper No. 2011-24-0067, 2011.
9. Tree, D. R. and Svensson, K. I., "Soot Processes in Compression Ignition Engines", Progress in Energy and Combustion Science, **33** (3), pg. 272-309, 2007.
10. Singh, G. in: *Doe Perspective: Government Role in Advanced Combustion Engine R&D*, SAE High Efficiency IC Engines Symposium Detroit, MI, 2011; Detroit, MI, 2011.